

SUBSONIC AND SUPERSONIC FLOW AROUND  
NONAXISYMMETRIC FUSELAGES

H. Rothman

(NASA-TT-F-14547) SUBSONIC AND SUPERSONIC N72-32302  
FLOW AROUND NONAXISYMMETRIC FUSELAGES H.  
Rothman (Scientific Translation Service)  
Sep. 1972 20 p CSCI 20D Unclass  
G3/12 41814

Translation of: " Die Umströmung nichtrotationssym-  
metrischer Rümpfe in Unter- und Überschall," Zeits-  
chrift für Flugwissenschaften, Vol. 20, March, 1972,  
pp. 98 - 105.



NATIONAL AERONAUTICS AND SPACE ADMINISTRATION  
WASHINGTON, D. C. 20546 SEPTEMBER 1972

# SUBSONIC AND SUPERSONIC FLOW AROUND NONAXISYMMETRIC FUSELAGES\*

Hermann Rothman\*\*

ABSTRACT. Description of a method for calculating the flow about nonaxisymmetric bodies in subsonic and supersonic flow. The bodies are constructed by means of the streamlines on their surface. Source, dipole, and quadrupole singularities are assumed on a curved camberline; the differential equations for the streamlines are derived and are numerically integrated. At the tip of the body, which is the initial point of the integration as well as a singular point of the differential equations, the problem can be solved by a transformation to "conical" coordinates. Different cross-sections and longitudinal sections of the body can be produced by varying the source, dipole, and quadrupole strengths as well as the "camber" of the camberline. This method seems to be particularly suitable in cases in which the streamlines are of interest. Using this method, the pressure distribution and the air forces on bodies can be determined.

## 1. INTRODUCTION

/98\*\*\*

The theory of flow around aerodynamic bodies has gained in importance over the last few years. Primarily, non-axially symmetric body shapes are of great interest for modern high performance aircraft. The method of superposition of singular integrals in the solution of the linearized gasdynamic fundamental equations, which was first used by Th. von Kármán [1] and M.M. Munk [2,3], has

---

\* Short version of a dissertation of the author approved by the Mechanical Engineering Department of the Technical University Vienna.

\*\* Aachen. Institute for Theoretical Gas Dynamics (Director: Prof. Dr. Phil K. Oswatitsch of the German Research and Test Facility for Aerodynamics and Space Flight (DFVLR).)

\*\*\* Numbers in the margin indicate pagination in the original foreign text.

been extended and improved in various ways.

The calculation of the axisymmetric flow goes back to the work of F. Weinig [4] and M.M. Munk [3]. They replaced the body by a source or dipole distribution along the x-axis and satisfied the boundary conditions along the body axis in an approximate way. This method was then extended to wings having small aspect ratio by F. Keune [5,6], K. Oswatitsch [6], W.T. Lord and G.G. Brebner [7], M.C. Adams and W.R. Sears [8], J. Weber [9] and K. Gersten [10]. M.D. Van Dyke [11,12] was able to improve the results using a second order theory. Most of these papers deal with the "inverse" problem in which the body shape is determined from a specified singularity distribution. J.F. Moran [13] attacked the direct problem, based on the work of F. Vandrey [14] and L. Landweber [15], in which the body cross section is developed into a power series and the source distribution is found by means of an iteration. /99

M.M. Munk [2] and R.T. Jones [16] and G.V. Ward [17] suggested another method of solution. They were able to show that for slender bodies, the flow can be approximated by means of a two-dimensional potential equation. Two methods were used for the two-dimensional problem: conformal mapping as well as the method of covering the body contour with singularities, first used by G.V. Ward [17]. D. Hummel [18] gives a detailed description of this method.

This paper has been stimulated by a theory given by K. Oswatitsch [19] for the calculation of flow surfaces in a steady, three-dimensional flow. Arbitrary flow surfaces are selected in a parallel basic flow and its deformation is determined using a perturbation calculation in a slightly perturbed flow. When this method is extended to non-axisymmetric bodies, it was found that the requirement for a small perturbation of the flow surface gradient cannot be satisfied in the vicinity of the axis.

In the present paper we, therefore, give a new method of calculating aerodynamic bodies in a frictionless flow free of heat conduction using streamlines along their surface. A covering by singularities consisting of sources, dipoles and quadrupoles over a prescribed skeleton line is assumed. The

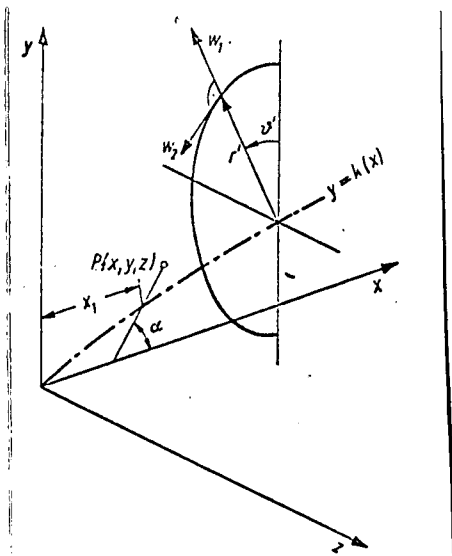


Fig. 1. Specification of the  $x, r, \varphi$  coordinate system of the velocity components across the cross section as well as the upper limits in Equation 3.4).

differential equations for the streamlines are established and integrated numerically. Using the equivalence law of Oswatitsch and Keune [6], the calculation of the drag, lift and the region near acoustic velocity can be considerably simplified or can be reduced to a rotationally symmetric problem. The method can be transferred to special cases in which the streamline course is of interest, such as, for example, in non-steady flows or in boundary layer theory.

## 2. DERIVATION OF THE BASIC EQUATIONS

In the following, it is assumed that the basic flow is in the  $x$ -direction, even for problems at which there is incidence. Let  $\Psi = \text{const}$  be a flow surface. The following condition follows from the condition that the velocity vector must lie along this surface:

$$w \text{ grad } \Psi = 0. \quad (2.1)$$

The characteristic line of such a differential equation is the streamline:

$$x(t), y(t), z(t), \quad (2.2)$$

where  $t$  can be an arbitrary parameter. From  $\Psi = \text{const}$ , by differentiation, it follows that

$$\frac{d\Psi}{dt} = \frac{\partial \Psi}{\partial x} x_t + \frac{\partial \Psi}{\partial y} y_t + \frac{\partial \Psi}{\partial z} z_t = 0, \quad (2.3)$$

and Equations (2.1) and (2.3) lead to the following system of differential equations for the streamlines

$$\begin{cases} x_t = f(x, y, z) u, \\ y_t = f(x, y, z) v, \\ z_t = f(x, y, z) w. \end{cases} \quad (2.4)$$

The function  $f(x, y, z)$  can be selected arbitrarily.  $u, v, w$  are the dimensionless perturbation velocity components, made dimensionless by means of the incident velocity  $u_\infty$ . If we then ignore the perturbation velocity  $u$  compared with the incident velocity  $u_\infty$ , as is done when boundary conditions are treated in the linearized subsonic and supersonic problems, then Equation (2.4) can be simplified and with  $t = x$  and  $f(x, y, z) = 1$  we find:

$$\left. \begin{aligned} \frac{dy}{dx} = v, \quad \frac{dz}{dx} = w. \end{aligned} \right\} \quad (2.5)$$

In the subsonic range, the flow conditions in the immediate vicinity of the stagnation point are not correctly represented when this simplification is introduced. However, this approximation is quite good for fuselages. For the further development, it is more convenient to use the coordinates shown in Figure 1.

The following relationships hold for the new coordinates  $(x, r', \vartheta')$ :

$$r'^2 = [y - k(x)]^2 + z^2, \quad \vartheta' = \arctan \frac{z}{y - k(x)}, \quad (2.6)$$

where the covered line is given by  $y = k(x)$ ,  $z = 0$ . It was found that a continuous distribution of singularities along  $y = k(x)$  is more advantageous than covering the  $x$ -axis. It is then also possible to have incidence angles larger than the tip angle. Using the transformation equations for the velocity components shown in Figure 1

$$\left\{ \begin{aligned} w_1 &= v \cos \vartheta' + w \sin \vartheta', \\ w_2 &= -v \sin \vartheta' + w \cos \vartheta' \end{aligned} \right\} \quad (2.7)$$

we obtain the following system of differential equations for the streamlines from (2.5) and the derivative of Equation (2.6) with respect to  $x$ :

/100

$$\frac{dr'}{dx} = w_1 - k_x(x) \cos \vartheta', \quad (2.8)$$

$$\frac{d\vartheta'}{dx} = \frac{1}{r'} (k_x \sin \vartheta' + w_2). \quad (2.9)$$

### 3. CALCULATION OF THE VELOCITY COMPONENTS IN THE VICINITY OF THE AXIS

By arranging source, dipole and quadrupole singularities of various intensities along the curve skeleton line, it becomes possible to influence the cross sectional shape of the body to be defined. Assuming small perturbations in the irrotational flow, the following equations hold:

$$(1 - M_\infty^2) \frac{\partial u}{\partial x} + \frac{\partial v}{\partial y} + \frac{\partial w}{\partial z} = 0, \quad (3.1)$$

$$\frac{\partial u}{\partial y} - \frac{\partial v}{\partial x} = 0, \quad \frac{\partial u}{\partial z} - \frac{\partial w}{\partial x} = 0, \quad \frac{\partial v}{\partial y} - \frac{\partial w}{\partial z} = 0, \quad (3.2)$$

where the velocity vector is the gradient of a potential  $\phi(x, y, z)$  according to Equation (3.2).

We will first start with the source solution. As the initial potential we use the following integral representations in the subsonic and supersonic ranges:

$$M_\infty < 1: \varphi_0 = -\frac{1}{4\pi} \int_0^1 Q_s(\xi) \times \frac{d\xi}{V(x-\xi)^2 + \beta^2 [(y-k(\xi))^2 + z^2]}, \quad (3.3)$$

$$M_\infty > 1: \varphi_0 = -\frac{1}{2\pi} \int_0^1 F_s(\xi) \times \frac{d\xi}{V(x-\xi)^2 - \cot^2 \alpha [(y-k(\xi))^2 + z^2]}, \quad (3.4)$$

where  $\beta = \sqrt{1 - M_\infty^2}$  and  $\cot \alpha = \sqrt{M_\infty^2 - 1}$  |  $M_\infty$  is the Mach number of the incident flow and  $F(x)$  and  $Q(x)$  are proportional to the cross sectional area. The upper integration limit  $x_1$  will be described in more detail when we deal with the subsonic case.

It is more convenient to set  $\beta = 1$  for the remainder of the treatment. The results can then be transferred without difficulty to arbitrary Mach numbers using the Prandtl-Glauert analogy. When one approaches the covered axis  $y \rightarrow k(x)$ ,  $z \rightarrow 0$ , the integrands in (3.3) and (3.4) increase indefinitely.

In order to investigate the behavior in the vicinity of the axis,  $k(\xi)$  is expanded at the point  $\xi = x$ :

$$k(\xi) = k(x) + k_x(x)(\xi - x) + \frac{1}{2} k_{xx}(x)(\xi - x)^2, \quad (3.5)$$

and the integral (3.3) is split into two parts by adding  $Q_x(x)$ , similar to what was done in a paper by Oswatitsch and Keune [6]. Assuming that  $k(x) \ll 1$ , which must already be prescribed due to the assumption of small perturbations, we then obtain:

$$\begin{aligned} \eta_0 = & -\frac{Q_r(x)}{4\pi} \times \\ & \times \int_0^1 \frac{d\xi}{\sqrt{(x-\xi)^2 - 2k_r(y-k(x))(\xi-x) + r'^2}} - \\ & - \frac{1}{4\pi} \int_0^1 \frac{Q_r(\xi) - Q_r(x)}{\sqrt{(x-\xi)^2 - 2k_r(y-k(x))(\xi-x) + r'^2}} d\xi. \end{aligned} \quad (3.6)$$

The second integral remains regular during the transition to the limit  $r' \rightarrow 0$ . The first integral can be simply integrated:

$$\begin{aligned} \eta_0 = & \frac{Q_r(x)}{4\pi} \ln \frac{4x(1-x)}{r'^2} - \\ & - \frac{1}{4\pi} \int_0^1 \frac{Q_r(\xi) - Q_r(x)}{|\xi - x|} d\xi. \end{aligned} \quad (3.7)$$

We find the following results for the velocity components:

$$\begin{aligned} v = & \frac{Q_r(x)}{2\pi r'} \cos \vartheta', \quad w = \frac{Q_r}{2\pi r'} \sin \vartheta', \\ w_1 = & \frac{Q_r}{2\pi r'}, \quad w_2 = 0. \end{aligned} \quad (3.8)$$

We require the  $u$  component of the velocity for the further calculation of the pressure coefficient. It is obtained from (3.3) by differentiation with respect to  $x$ :

$$u = \frac{1}{4\pi} \int_0^1 \frac{Q_r(\xi)(x-\xi)d\xi}{[(x-\xi)^2 - 2k_r(\xi-x)(y-k) + r'^2]^{3/2}}. \quad (3.9)$$

After substitution of the Taylor series development (3.5) and expanding the numerator  $[y - k(x)] k_x(x)$ , (3.9) can be divided into two partial integrals  $I_1$  and  $I_2$ :

$$I_1 = -\frac{1}{4\pi} \times \left. \begin{aligned} & \times \int_0^1 \frac{Q_x(\xi) [(\xi - x) - (y - k) k_x]}{[(x - \xi)^2 - 2(\xi - x)(y - k) k_x + r'^2]^{3/2}} d\xi \end{aligned} \right\} \quad (3.10)$$

$$I_2 = -\frac{1}{4\pi} \times \left. \begin{aligned} & \times \int_0^1 \frac{Q_x(\xi) (y - k) k_x}{[(x - \xi)^2 - 2k_x(\xi - x)(y - k) + r'^2]^{3/2}} d\xi \end{aligned} \right\} \quad (3.11)$$

After a partial integration (because  $Q_x(0) = Q_1(1) = 0$  the integrated part vanishes), the integral  $I_1$  becomes an integral having the same form as (3.3). The second integral can be treated just like (3.6) by adding and subtracting  $Q_x(x)$ . We finally obtain the following results for the  $u$  component:

$$u = -\frac{1}{4\pi} Q_{xx} \ln \frac{4x(1-x)}{r'^2} - \frac{1}{2\pi} Q_x \frac{k_x \cos \theta'}{r'} - \frac{1}{4\pi} \int_0^1 \frac{Q_{xx}(\xi) - Q_{xx}(x)}{|\xi - x|} d\xi. \quad (3.12)$$

The second expression shows the influence of the covering of a curved line that has the same form as the  $u$  component of an incidence potential with  $k_x$  as the local cross section incident flow. /101

### 3.1. Supersonic Case

As can be seen from Figure 1, the upper limit  $x_1$  is found by setting the denominator in (3.4) equal to:

$$(x - x_1)^2 = \{[y - k(x_1)]^2 + z^2\} \cot^2 \alpha. \quad (3.13)$$



For  $r' \rightarrow 0$ , (3.13) can be simplified by means of a Taylor expansion at the point  $x = x_1$  and  $x_1$  can be explicitly calculated:

$$x_1 = x - \left( 1 + k_x \cot \alpha \cos \vartheta' + \frac{1}{2} k_x^2 \cot^2 \alpha \cos^2 \vartheta' \right) r' \cot \alpha. \quad (3.14)$$

By expansion of the upper limit and a similar simplification of the integrand as was done in the subsonic case, the properties of the integral (3.4) are not changed. Corresponding to (3.7), we obtain the following result:

$$\varphi_0 = \frac{1}{2\pi} F_x(x) \ln(\cot \alpha r') + S(x), \quad (3.15)$$

where  $S(x)$  contains all terms which only depend on  $x$ . The following is then found for the velocity components:

$$v = \frac{1}{2\pi r'} F_x(x) \cos \vartheta', \quad w = \frac{1}{2\pi r'} F_x \sin \vartheta'. \quad (3.16)$$

For the calculation of the  $u$  component, the denominator of (3.4) is again developed into a series and expanded to a complete square. The potential, by means of the transformation

$$\lambda = \text{Arcosh} \left( \frac{x - \xi}{\cot \alpha r'} - k_x \cot \alpha \cos \vartheta' \right) \quad (3.17)$$

is transformed into the form:

$$\varphi_0 = \frac{1}{2\pi} \int_a^0 F_x \left( x - r' k_x \cot^2 \alpha \cos \vartheta' - r' \cot \alpha \cosh \lambda \right) d\lambda, \quad (3.18)$$

$$a = \text{Arcosh} \left( \frac{x}{r' \cot \alpha} - k_x \cot \alpha \cos \vartheta' \right).$$

The integrand vanishes at the lower limit, so that the derivative with respect to  $x$  and the following reverse transformation become very simple:

$$u = -\frac{F_x}{2\pi r'} k_x \cos \vartheta' + \frac{F_{xx}}{2\pi} \ln \left( \cot \alpha \frac{r'}{2x} \right) - \frac{1}{2\pi} \int_0^x \frac{F_{xx}(\xi) - F_{xx}(x)}{|\xi - x|} d\xi. \quad (3.19)$$

A comparison of (3.16) and (3.15) with (3.8) and (3.7), respectively, shows that the  $v$  and  $w$  component as well as the part of the potential dependent on  $y, z$  are identical for the subsonic and supersonic case. This agreement is also a direct consequence of the theory of Jones. The cross section flow does not depend on the Mach number within the framework of our approximation. Only the part of the source potential which depends on  $y, z$  is important for the derivation of the higher singularities. Therefore, in the remaining calculation we can restrict ourselves to the subsonic case.

### 3.2. Dipole and Quadrupole Singularity

The dipole and quadrupole potential is given by the second and third term of the general solution of (3.1):

$$\varphi = \sum_{k=0}^{\infty} r'^k \left[ \cos k \vartheta' \times \right. \\ \left. \times \left( \frac{1}{r'} \frac{\partial}{\partial r'} \right)^k \int_0^1 \frac{f_k(\xi)}{\sqrt{(x-\xi)^2 + \beta^2 r'^2}} d\xi \right]. \quad (3.20)$$

It can be shown that differentiation and transfer to the limit ( $r' \rightarrow 0$ ) can be interchanged in (3.3). We obtain the following for the dipole or quadrupole potential in the vicinity of the axis from (3.7):

$$\varphi_D = \frac{M(x)}{2\pi r'} \cos \vartheta', \quad \varphi_Q = -\frac{1}{\pi} N(x) \frac{\cos 2\vartheta'}{r'^2}, \quad (3.21)$$

where  $M(x)$  is the dipole moment and  $N(x)$  is the quadrupole intensity. From (3.21), the following is obtained for the dipole velocity components:

$$u_D = \frac{M_x(x)}{2\pi r'} \cos \vartheta' + \frac{M k_x}{2\pi r'^2} \cos 2\vartheta', \quad (3.22)$$

$$w_{1D} = -\frac{M}{2\pi r'^2} \cos \vartheta', \quad w_{2D} = -\frac{M}{2\pi r'^2} \sin \vartheta' \quad (3.23)$$

and the following is obtained for the quadrupole velocity components:

$$u_l = -\frac{1}{\pi} N_x(x) \frac{\cos 2\vartheta'}{r'^2} - \left. \begin{aligned} & - \frac{2N k_r}{\pi r'^3} \cos \vartheta' (\cos^2 \vartheta' - 3 \sin^2 \vartheta') \end{aligned} \right\} \quad (3.24)$$

$$w_{1l} = \frac{2}{\pi r'^3} N \cos 2\vartheta', \quad w_{2l} = \frac{2}{\pi r'^3} N \sin 2\vartheta'. \quad (3.25)$$

From (3.7) it is seen that the x-dependence of the potential in the vicinity of the axis is the same as for a body of revolution having the same cross sectional surface  $Q(x)$ . This theorem of an "equivalent" body of revolution was first given by Oswatitsch and Keune [6] in the treatment of bodies at zero incidence within the area of linearization of the gas dynamic equations. It was first given by Oswatitsch [20] for the velocity range near sonic velocity.

#### 4. CONICAL FLOW AT THE BODY TIP

Except for certain special cases, for example, such as the body of revolution at incidence, the two differential equations for the streamlines (2.8) and (2.9) can only be integrated numerically. The initial conditions are specified at the body tip:  $x = 0: r' = 0, \vartheta' = \vartheta'_0$ . The streamlines originate at the body tip and the integration difficulties consist of the fact that the system of differential Equations (2.8) or (2.9), respectively, has a singular point, a bifurcation point, there. The problem can be treated as a conical problem within a small vicinity of the tip and can be solved analytically by means of a Taylor expansion or corresponding trial solutions for the functions  $Q(x)$ ,  $M(x)$ ,  $N(x)$ ,  $k(x)$ .

If the individual singularity components are introduced in (2.8) or (2.9) for the velocity components  $w_1$  and  $w_2$ , then the following two differential equations are obtained:

$$\frac{dr'}{dx} = \frac{Q_r}{2\pi r'} - k_r \cos \vartheta' - \left. \begin{aligned} & - \frac{M}{2\pi r'^2} \cos \vartheta' + \frac{2N}{\pi r'^3} \cos 2\vartheta' \end{aligned} \right\} \quad (4.1) \quad \underline{/102}$$

$$\frac{d\vartheta'}{dx} = \left( \frac{k_r}{r'} - \frac{M}{2\pi r'^3} \right) \sin \vartheta' + \frac{2N}{\pi r'^4} \sin 2\vartheta'. \quad (4.2)$$

The following trial solutions are used for the covered line as well as for the individual singularity intensities:

$$\left. \begin{aligned} Q(x) &= a_0^2 \tau^2 \pi x^2 (1-x)^2, \\ M(x) &= -2 a_D \tau^3 \pi x^2 (1-x)^2 (1-2x), \\ N(x) &= \frac{a_I}{2} \tau^4 \pi x^3 (1-x)^3 (1-2x), \\ k(x) &= a_k \tau x (1-x). \end{aligned} \right\} \quad (4.3)$$

In certain special cases other trial solutions will have to be used. The free selection of the individual singularity intensities is a consequence of the "inverse" problem formation, i.e., it is not the body but the singularity covering law which is prescribed.

In the vicinity of the body tip, Equation (4.3) can be simplified by means of an expansion for  $x$ :

$$\left. \begin{aligned} Q(x) &= a_0^2 \tau^2 \pi x^2, & k(x) &= a_k \tau x, \end{aligned} \right\} \quad (4.4)$$

$$\left. \begin{aligned} M(x) &= -2 a_D \tau^3 \pi x^2, & N(x) &= \frac{a_I}{2} \tau^4 \pi x^3, \end{aligned} \right\} \quad (4.5)$$

and from (4.1) and (4.2), respectively, we obtain:

$$\left. \begin{aligned} \frac{dr'}{dx} &= a_0^2 \frac{x}{r'} - \\ &\quad - \left( a_k - a_D \frac{x^2}{r'^2} \right) \cos \vartheta' + a_I \frac{x^3}{r'^3} \cos 2 \vartheta', \end{aligned} \right\} \quad (4.6)$$

$$\frac{d\vartheta'}{dx} = \left( \frac{a_k}{r'} + a_D \frac{x^2}{r'^2} \right) \sin \vartheta' + a_I \frac{x^3}{r'^4} \sin 2 \vartheta'. \quad (4.7)$$

The equations have already been divided by the thickness parameter  $\tau$ . In the following we will always use  $r'$  for  $r'/\tau$ . It is now expedient to introduce a conical coordinate  $\bar{\xi}$ :

$$\left[ \frac{r'}{x} = \bar{\xi} = a_0 \bar{\xi}, \quad \frac{dr'}{dx} = \bar{\xi} + x \frac{d\bar{\xi}}{dx} \right] \quad (4.8)$$

and to transform (4.6) to this new coordinate:

$$\left[ x \frac{d\bar{\xi}}{dx} = \frac{1}{\bar{\xi}} - A_k \cos \vartheta' + \right. \quad (4.9)$$

$$\left. + \frac{A_D}{\bar{\xi}^2} \cos \vartheta' + \frac{A_I}{\bar{\xi}^3} \cos 2 \vartheta' - \bar{\xi}, \right]$$

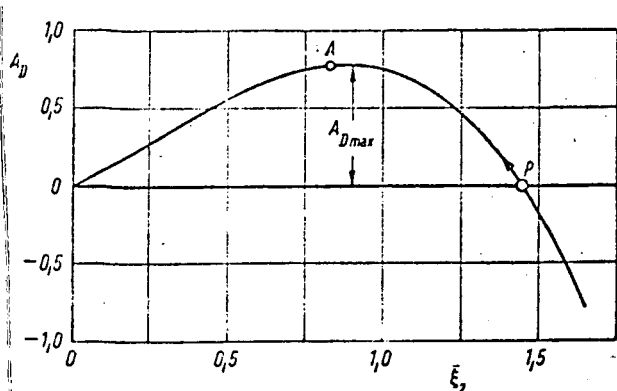


Fig. 2. Source-dipole singularity; solution of the equation  $A_D = F(\xi_2)$

$$A_k = 0.75$$

Reproduced from  
best available copy.



For simplicity we will confine our discussion of (4.10) to a source dipole covering ( $A_f = 0$ ). The treatment with an additional quadrupole singularity as well as with a pure source flow ( $A_D = A_f = 0$ ) is equivalent.  $x = 0$  is a singular point of (4.10). If the differential quotient is to remain finite, then the right side must vanish. We obtain two cubic equations for  $\bar{\xi}_1$  ( $\vartheta' = 0$ ) and  $\bar{\xi}_2$  ( $\vartheta' = \pi$ ) (lower sign):

$$\bar{\xi}_1^3 \pm A_k \bar{\xi}_1^2 - \bar{\xi}_1 \pm A_D = 0. \quad (4.11)$$

Figure 2 shows the inverse function  $A_D = A_D(\bar{\xi}_2)$ . The negative curve part

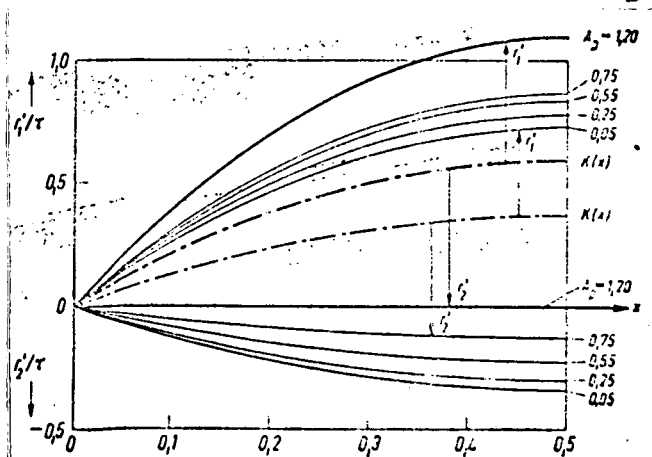


Fig. 3. Source-dipole singularity; stream lines for various dipole and source strengths. Thin lines:  $A_k = 0.75$ , thick lines:  $A_k = 1.2$ .

where  $A_k$ ,  $A_D$  and  $A_f$  are given by

$a_k/a_0$ ,  $a_D/a_0^3$  and  $a_f/a_0^4$ , respectively.

We will first consider the top and bottom streamlines  $\vartheta' = 0$  (upper sign in (4.10) and  $\vartheta' = \pi$  (lower sign). Then (4.7) is satisfied identically. The following ordinary differential equation is obtained from (4.9)

$$x \frac{d\bar{\xi}}{dx} = \frac{1}{\bar{\xi}} \mp A_k \pm \frac{A_D}{\bar{\xi}^2} + \frac{A_f}{\bar{\xi}^3} - \frac{1}{\bar{\xi}}. \quad (4.10)$$

( $A_D < 0$ ) corresponds to dipoles which blow downwards and are not of any consequence in the further discussion. The point P ( $A_D = 0$ ) corresponds to the source flow. As the dipole intensity is increased,  $\bar{\xi}_2$  continues to become smaller, i.e., the lower streamline  $\vartheta' = \pi$  approaches the covered axis given by  $\bar{\xi}_2 = 0$ .

Figure 3 shows the two streamlines  $\vartheta' = 0$  and  $\vartheta' = \pi$  for various values of  $A_D$  and  $A_k$ . For  $A_D > A_{D_{\max}}$

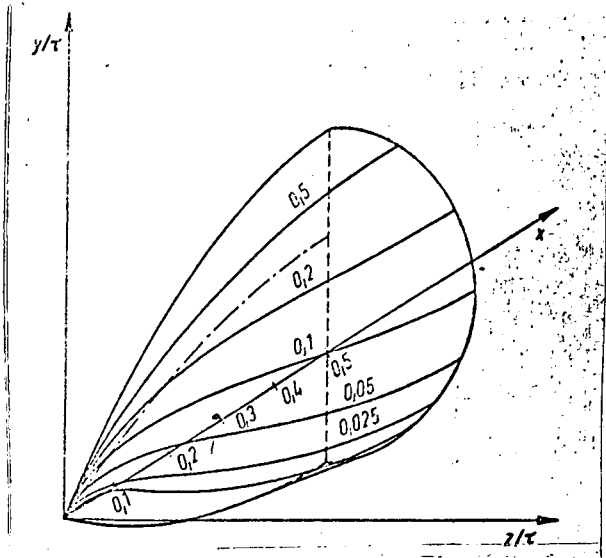


Fig. 4. Streamlines and bodies for a source singularity,  $A_k = 0.75$ .

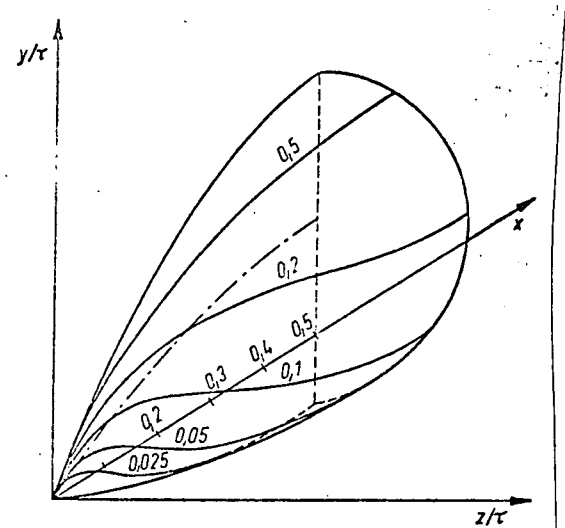


Fig. 5. Streamlines and bodies for a source dipole singularity,  $A_k = 0.75$ ,  $A_D = 0.55$ .

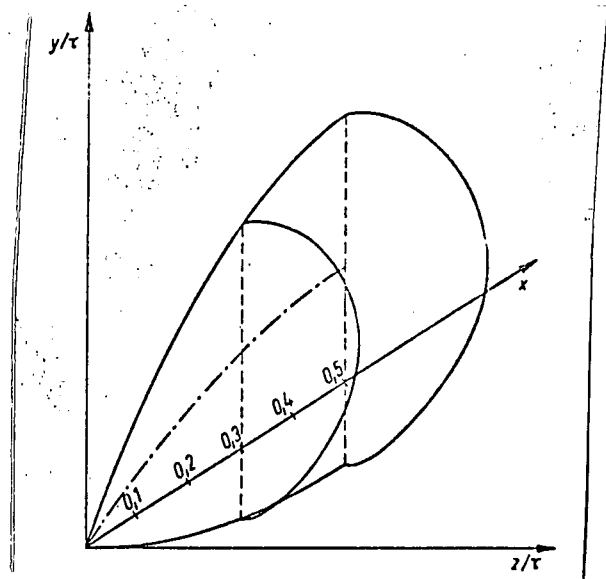


Fig. 6. Cross section distribution for a source dipole quadrupole singularity,  $A_k = 0.75$ ,  $A_D = 0.55$ ,  $A_f = 0.2$ .

no real positive solution exists for  $\bar{\xi}_2$ . Therefore, it is not possible to lift the lowest body streamline up to the x-axis or above it by increasing the dipole intensity, if the source intensity and covered line are prescribed arbitrarily. This can only be done by a suitable selection of the source dipole strength or the covered line. Figure 3 shows an example of this by a thick line. Comparison of the  $v$  or  $w_1$  components of the source and the dipole (3.8) or (3.23), respectively, shows that the dipole term is dominant in the vicinity of the axis.

In addition to the "external" solution described, Figure 2 also contains a "internal" solution (the part of the curve with positive inclination), which has no physical meaning.

In order to solve the general case (4.6) or (4.7), the last equation is transformed to the  $\bar{\xi}$  coordinate and one finally obtains the following after introducing a new coordinate  $\eta = \cos \theta$ :

$$\left[ \frac{d\bar{\xi}}{d\eta} = \frac{\bar{\xi} [\bar{\xi}^2 - A_k \bar{\xi}^2 \eta + A_D \bar{\xi} \eta + A_I (2\eta^2 - 1) - \bar{\xi}^4]}{(\eta^2 - 1) [\bar{\xi} (A_k \bar{\xi}^2 + A_D) + 2\eta A_I]} \right] \quad (4.12)$$

From (4.7) it can be seen that the angle must satisfy  $|\theta'| = 0$  or  $\eta = 1$  at the body tip ( $x = 0$ ,  $r' = 0$ ) for all streamlines, except for the lowest one  $|\theta| = \pi$ . If we set the numerator in (4.12) equal to zero, then we obtain an equation for determining  $\bar{\xi}_1$ . This makes the initial condition  $\eta = 1$ :  $\bar{\xi} = \bar{\xi}_1$  a simultaneous singular point of (4.12). In order to obtain an analytical solution in the vicinity of this point, we use the following trial solution:

$$\bar{\xi} = \bar{\xi}_1 + C(1 - \eta)^a \quad (4.13)$$

By comparing coefficients, we obtain the following from (4.12) for the constants  $a$  and  $C$ :

$$a = 1, \quad C = \frac{\bar{\xi}_1 (A_k \bar{\xi}_1^3 - A_D \bar{\xi}_1 - 4 A_I)}{6 A_k \bar{\xi}_1^3 + 3 A_I - 3 \bar{\xi}_1^2 + 5 \bar{\xi}_1^4} \quad (4.14)$$

We must still find a corresponding solution for  $x = x(\eta)$  in the vicinity of the body tip. The following differential equation can be derived from (4.10) and (4.12)

$$\frac{dx}{d\eta} = \frac{x \bar{\xi}^4}{(\eta^2 - 1) [\bar{\xi} (A_k \bar{\xi}^2 + A_D) + 2\eta A_I]} \quad (4.15)$$

After introducing the trial solution (4.13) we can integrate without any difficulty:

$$x = K_3 (1 - \eta)^m, \quad m = \frac{\bar{\xi}_1^4}{2 [\bar{\xi}_1 (A_k \bar{\xi}_1^2 + A_D) + 2 A_I]} \quad (4.16)$$

By a corresponding selection of the free integration constant  $K_3$ , we find that the individual streamlines can be transformed into each other by compression with is a characteristic property of conical flows.

## 5. GENERAL FLOWS

If these trial solutions (4.3) are introduced into (4.1) and (4.2), the following equations are obtained for the streamlines:

$$\left. \begin{aligned} \frac{dy'}{dx} = & \frac{a_0^2 x (1-x) (1-2x)}{r'} + \\ & + (1-2x) \left\{ \left[ -a_k + \frac{a_{11} x^2 (1-x)^2}{r'^2} \right] \cos \vartheta' + \right. \\ & \left. + \frac{a_l x^3 (1-x)^3}{r'^3} \cos 2\vartheta' \right\}, \end{aligned} \right\} \quad (5.1)$$

$$\left. \begin{aligned} \frac{d\vartheta'}{dx} = & \sin \vartheta' (1-2x) \left[ \frac{a_k}{r'} + \right. \\ & \left. + \frac{a_{11} x^2 (1-x)^2}{r'^3} + \frac{2 a_l x^3 (1-x)^3}{r'^4} \cos \vartheta' \right], \end{aligned} \right\} \quad (5.2)$$

These differential equations can only be integrated numerically in a general case. The analytical solution is attached to it in the vicinity of the singular initial point. It is found that the solution is only modified slightly by displacing the transition point. Figure 4 shows the streamlines for a source covering. It is an axonometric representation in which body cross sections in the planes  $x = \text{const}$  remain undistorted. We can also observe the emergence of all streamlines from the tip at angle zero. Figure 5 shows a body with an additional dipole distribution. Because of the dipoles, the streamlines are pushed onward faster and the entire body is lifted upwards. Figure 6 shows the influence of a quadrupole covering. The two body cross sections shown are considerably more slender than those shown in the previous two figures. /104

### 5.1. Calculation of the Pressure Distribution

In order to calculate the pressure coefficients  $c_p$ , we must consider the quadratic terms in  $v$  and  $w$  already in the first approximation, similar to what occurs in the rotationally symmetric case:

$$c_{pG} = -2 u_G^2 - v_G^2 - w_G^2. \quad (5.3)$$

The subscript G refers to the total value. In accordance with the three singularity components of the total velocity components  $u_G$ ,  $v_G$ ,  $w_G$ , we will also split the pressure coefficients into three parts:



$$c_{pi} = c_p + c_{pi} + c_{pi} \quad (5.4)$$

It should be noted that the mixed quadratic terms must also be included in the last two components (such as  $v v_D$  in the dipole component  $c_{pD}$ ,  $v_D v_f$  in the quadrupole component  $c_{pf}$ ). If we substitute the corresponding equations for the velocity components, then we find:

Source:

$$c_p = \frac{1}{2\pi} Q_{xx} \ln \frac{4x(1-x)}{r'^2} + \frac{1}{\pi} Q_x \frac{k_x \cos \vartheta'}{r'} - \frac{Q_x^2}{4\pi^2 r'^2} + \frac{1}{2\pi} \int_0^1 \frac{Q_{xx}(\xi) - Q_{xx}(x)}{|\xi - x|} d\xi \quad (5.5)$$

Dipole:

$$c_{pD} = -\frac{M}{\pi r'} \cos \vartheta' - \frac{M^2}{4\pi^2 r'^4} - \frac{M k_x \cos 2\vartheta'}{\pi r'^2} + \frac{Q_x M}{2\pi^2 r'^3} \cos 2\vartheta' \quad (5.6)$$

Quadrupole:

$$c_{pI} = \frac{2N_x \cos 2\vartheta'}{\pi r'^2} + \frac{4N k_x}{\pi r'^3} (\cos^2 \vartheta' - 3 \sin^2 \vartheta') \cos \vartheta' - \frac{4N^2}{\pi^2 r'^6} - \frac{2Q_x N}{\pi^2 r'^4} \cos 2\vartheta' + \frac{2MN}{\pi^2 r'^5} \cos \vartheta' \quad (5.7)$$

The pressure coefficient plotted in Figure 7 was calculated using these formulas. The body used is the one shown in Figure 5.

## 5.2. Calculation of the Lift

As is well known, the lift can be calculated according to two methods. This can be done by integration of the pressure coefficient over the body surface or using a control surface which follows from the momentum theorem:

$$A = \int_0^1 \int_0^{2\pi} [\rho w_n v + (p - p_\infty) \cos(n, y)] r_0' d\vartheta' dx \quad (5.8)$$

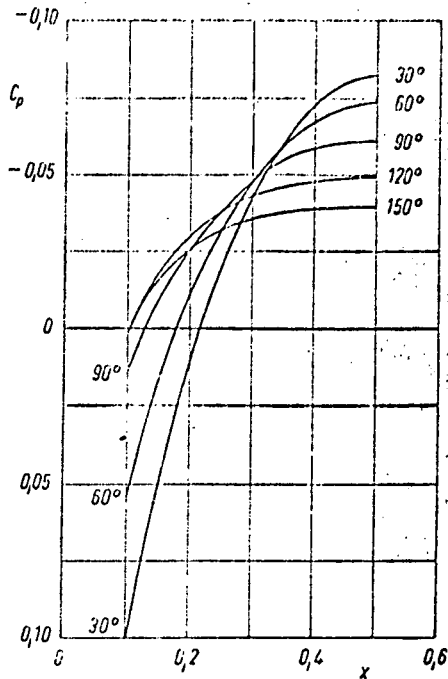


Fig. 7. Pressure distribution of the body shown in Figure 5 for source-dipole singularity,  $A_k = 0.75$ ,  $A_D = 0.55$ .

It is expedient to select a small cylindrical surface with the radius  $r'_0$  around the covering axis as the control surface. In the remainder of the calculation we can restrict ourselves to source-dipole singularities. It is easily shown that the quadrupole does not make a contribution based on the orthogonal relationships of trigonometric functions. For the pressure term  $(p - p_\infty)$  we can substitute the pressure coefficient multiplied by the incident stagnation pressure  $q_\infty$ . Using the formula for the velocity component in the direction of the surface normal

(5.9)

we obtain the final result:

$$A = 2 q_\infty \int_0^1 \int_0^{2\pi} \left[ -\frac{Q_x k_x}{2\pi r'_0} (1 + \cos^2 \vartheta') + \frac{\cos^2 \vartheta'}{2\pi r'_0} (3 Q_x k_x - M_x) \right] r'_0 d\vartheta' dx. \quad (5.10)$$

We integrate over  $\vartheta'$  and the transition to the limit  $r'_0 \rightarrow 0$  gives the following simple relationship for the lift:

$$A = q_\infty M(1). \quad (5.11)$$

From this it can be seen that a source-sink distribution does not produce any lift as expected within the framework of our approximation. The dipole covering only produces a lift force under the assumption  $M(1) \neq 0$ . This result is already known from the theory of bodies of revolution. In our case, we have the further interesting result that the semibody given by (4.3) also has no lift because of  $M(1/2) = 0$ .

## 6. REFERENCES

1. Kármán, Th. von. Calculation of Pressure Distribution on Airship Hulls. Abhandlungen aus dem Aerodynamischen Institut der TH Aachen, No. 6, 1927, pp. 3 - 17.
2. Munk, M.M. The Aerodynamic Forces on Airship Hulls. NACA Rep. 184, 1923. /105
3. Munk, M.M. Fluid Mechanics, Part II. In: W.F. Durand (Publisher): Aerodynamic Theory. Vol. 1, Division C. Julius Springer, Berlin, 1934.
4. Weinig, F. Rapidly Converging Graphical Solution of Flow Problems Using Integral Equations. Z. techn. Physik., Vol. 9, 1928, pp. 39 - 43.
5. Keune, F. Low Aspect Ratio Wings with Small Thickness at Zero Life in Subsonic and Supersonic Flow. KTH Stockholm, Aero TN 21, 1952.
6. Keune, F. and K. Oswatitsch. Small Span Bodies at Zero Incidence in Subsonic and Supersonic Flow. Z. Flugwiss., Vol. 1, 1953, pp. 137 - 145.
7. Lord, W.T. and G.G. Brebner. Supersonic Flow Past Slender Pointed Wings with "Similar" Cross-sections at Zero Life. Aeron. Quart., Vol. 10, 1959, pp. 79 - 102.
8. Adams, M.C. and W.R. Sears. Slender Body Theory. Review and Extension. J. Aeron. Sci., Vol. 20, 1953, pp. 85 - 98.
9. Weber, J. Slender Delta Wings with Sharp Edges at Zero Life. RAE TN Aero 2508, 1957.
10. Gersten, K. Calculation of the Supersonic Flow Around Slender Wings at Zero Incidence. Z. angew. Math. Mech., Vol. 43, 1963, pp. T 130 - T 132.
11. Van Dyke, M.D. Subsonic Edges in Thin-wing and Slender-body Theory. NACA TN 3343, 1954.
12. Van Dyke, M.D. Second-order Slender-body Theory. Axisymmetric Flow. NASA Techn. Rep. R-47, 1959.
13. Moran, J.P. Line Source Distribution and Slender Body Theory. J. Fluid Mech., Vol. 17, 1963, pp. 285 - 304.
14. Vandrey, F. A Direct Iteration Method for the Calculation of the Velocity Distribution of Bodies of Revolution and Symmetrical Profiles. Admiralty Research Laboratory, Teddington, Rep. R 1/G/HY/12/2, 1951.

15. Landweber, L. The Axially Symmetric Potential Flow about Elongated Bodies of Revolution. David W. Taylor Model Basin, Rep. 761, 1951.
16. Jones, R.T. Properties of Low-aspect Ratio Pointed Wings at Speeds Below and Above the Speed of Sound. NACA TN 1032, 1946.
17. Ward, G.N. Supersonic Flow Past Slender Pointed Bodies. Quart. J. Mech. Appl. Math., Vol. 2, 1949, pp. 75 - 97.
18. Hummel, D. Calculation of Pressure Distribution Over Slender Aerodynamic Bodies Having Arbitrary Cross-sectional and Top View Shapes in Subsonic and Supersonic Flow. Dissertation TU Braunschweig, 1968. 1968 Yearbook of the DGLR, pp. 158 - 173.
19. Oswatitsch, K. Flow Surfaces in Slightly Perturbed Parallel Flows. Z. Flugwiss., Vol. 14, 1966, pp. 14 - 18.
20. Oswatitsch, K. Theoretical Work on Near-acoustic Flow at the Technical Flight Institute of the Royal Technical High School at Stockholm. Proceedings of the 8th International Congress of Theoretical and Applied Mechanics, Istanbul, 1952, pp. 261 - 262.
21. Rothmann, H. Flow Around Non-rotationally Symmetric Fuselages in Subsonic and Supersonic Flow. Dissertation TH Wien, 1969.
22. Oswatitsch, K. Gasdynamics. Springer-Verlag, Wien, 1952.

Translated for National Aeronautics and Space Administration under contract No. NASw 2035, by SCITRAN, P. O. Box 5456, Santa Barbara, California, 93108.